Journal of Advanced Pharmacy Research



Section B: Pharmaceutical Analytical & Organic Chemistry, Medicinal & Biochemistry

Unraveling the Anti-Cancer Potential of Eichhornia crassipes: An In Silico Analysis of CDK4/6 Inhibition through Drug-Likeness Screening, Molecular Docking, and ADMET Evaluation

Memunat Alake Bankole^{1,2*}, Owolabi Nurudeen Abiodun^{1,2}, Jimoh Salamah Mopelola^{1,3}, Ajadi Ibrahim⁴, Olatunji Idayat Omotolani¹, Olagoke Amudalah Opeyemi¹, Lawal Mariam¹, Bamidele Shukurat Opeyemi¹

ISSN: 2357-0547 (Print)

ISSN: 2357-0539 (Online)

*Corresponding author: Memunat A. Bankole. Department of Biochemistry, Ladoke Akintola University of Technology, Ogbomoso, Nigeria. Foresight Institute of Research and Translation, Ibadan, Nigeria. Tel: 08143997654

E-mail address: memunatbankole912@gmail.com

Submitted on: 12-04-2025; Revised on: 19-06-2025; Accepted on: 19-07-2025

To cite this article: Bankole, M. A, Abiodun, O. N.; Mopelola, J. S.; Ibrahim, A.; Omotolani, O. I.; Opeyemi, O. A.; Mariam, L; Opeyemi, B. S. Unraveling the Anti-Cancer Potential of Eichhornia crassipes: An In Silico Analysis of CDK4/6 Inhibition through Drug-Likeness Screening, Molecular Docking, and ADMET Evaluation. *J. Adv. Pharm. Res.* **2025**, *9* (4), 167-177. DOI: 10.21608/aprh.2025.374897.1310

ABSTRACT

Objective: This current study utilized in silico approach; drug-likeness screening, molecular docking, protein-ligand interactions analysis, and ADMET evaluation to assess the inhibitory potential of the compounds present in Eichhornia crassipes (water hyacinth) for cancer treatment with the targets CDK4/6. Methods: Computational approach was explored in our investigation. 57 compounds were selected from water hyacinth via literature and were subjected to drug-likeness screening via SwissADME online tool. The Pubchem Identification number (PID), 3D structures, and canonical SMILES of compounds used in this study were retrieved from PubChem server. Three-dimensional structure of CDK4/6 were downloaded from the RCSB Protein Data Bank (PDB). Thereafter, the compounds that passed the screening were further subjected to molecular docking analysis with Schrodinger suite to identify inhibitors with superior binding affinity for CDK4/6. The pharmacokinetic properties of the compounds with higher binding affinity were evaluated with ADMETLab server. Results: As a result, five compounds (CID 5280443, CID 3469, CID 689043, CID 5281691, and CID 10742) and three compounds (CID 5280666, CID 5280343, and CID 5280445) with higher binding affinity than the reference drugs emerged as top therapeutic prospects against CDK4 and 6 respectively. Three drug candidates CID 3469, CID 10742, and CID 689043 showed better ADMET profiles than the control drugs while the remaining five may show equal output. Conclusion: This study revealed 8 hit compounds from water hyacinth with better binding affinity compared to control drugs against CDK4/6 targets. In addition, three drug candidates CID 3469, CID 10742, and CID 689043 showed better ADMET profiles than the control drugs while the remaining five may show equal output. Following extensive experimental testing, these compounds may show potential as a viable cancer treatment.

Keywords: Cyclin dependent kinase, water hyacinth, in silico, cancer, ADMET

¹Department of Biochemistry, Ladoke Akintola University of Technology, Ogbomoso, Nigeria

²Foresight Institute of Research and Translation, Ibadan, Nigeria

³Department of Microbiology, University of Ilorin, Ilorin, Nigeria

⁴Department of Plant and Environmental Biology, Kwara State University, Malete, Nigeria

INTRODUCTION

Cancer is one of the most serious ailments that exist. It is categorized by its potential to be cell-destructive, infectious, or metastatic. These three features differentiate it from benign tumors, which grow in a self-limited manner and do not penetrate or spread ¹. The International Agency for Research on Cancer estimates that cancer resulted in 9.7 million deaths and 20 million new diagnoses worldwide in 2022, emphasizing the urgency for improved cancer management ². Protein kinases are employed as a possible pharmacological target in cancer therapy since they regulate about 80% of biological pathways, including the cell cycle's progression, transcription, DNA repair, and metabolic activities in several signaling cascades ³.

Merely five out of the twelve isoforms of CDKs, which are heteromeric serine/threonine protein kinases, have been demonstrated to directly regulate the cell cycle (CDK1–CDK7)⁴. In order for eukaryotic cells to produce and maintain DNA, the cell cycle must be regulated, and CDKs are vital to this process. The G1 phase (cell growth), S phase (DNA synthesis), G2 phase (cell division preparation), and M phase (cell division) are among the cell cycle phases that CDKs are involved in controlling. They ensure these stages take place in a structured and systematic way 5. During the S phase of the cell cycle, CDKs are essential for starting DNA replication, especially those linked to particular cyclins. DNA synthesis initiation is facilitated by the phosphorylation of target proteins, mediated by these enzymes. By controlling the expression of genes involved in apoptosis, or programmed cell death, CDKs also contribute to this process. In broad terms, effective DNA development and cell proliferation depend on the precise control of the cell cycle by cyclin-dependent kinases ⁶. CDK plays a significant role in cell cycle and its dysregulation results in unchecked cell division which is among the hallmarks of cancer. Thus, there has been interest in cancer research and therapeutic development to comprehend and target CDKs. Most cancer cells exhibit either direct or indirect CDK dysfunction ⁷.

Cyclin-CDKs pathway is essential in the regulation of the cell cycle. The activation of CDK4/6 by cyclin D triggers a cascade of cellular events, culminating in the phosphorylation of the retinoblastoma protein (Rb). This modification releases the transcription factor E2F, facilitating the expression of cell cycle-regulated genes and driving cells from the G1 phase into the S phase, thereby promoting cellular proliferation ⁸. The primary challenge in the therapeutic application of CDK4/6 inhibitors is that patients who show initial response to treatment frequently go on to develop resistance and eventually succumb to the disease. Furthermore, many tumors have intrinsic preexisting resistance to CDK4/6 inhibitors ⁹.

Eichhornia crassipes, a highly invasive aquatic plant belonging to the Pontederiaceae family, has been recognized for its diverse pharmacological properties ¹¹. This plant, native to Brazil, is prevalent in tropical and subtropical areas, notably in Southeast Asia, the southeastern United States, central and western Africa, and Central America ¹⁰. Water hyacinth significantly impacts both the environment and economy, leading to reduced water quality and biodiversity ¹⁰.

Notably, this water hyacinth exhibits a range of bioactivities. including anticancer. antioxidant. antimicrobial, and anti-inflammatory effects, making it a promising candidate for therapeutic applications ¹². Traditionally, it has been used to treat gastrointestinal issues like diarrhea, digestive disorders, and parasitic infections. The plant's therapeutic properties stem from numerous secondary metabolites, such as polyphenols, flavonoids, fatty acids, alkaloids, saponins, terpenoids, sterols, phenalene's, phenylphenalenes, quinones, anthraquinones, organic acids, carbohydrates, and other compounds¹³. Studies have demonstrated that secondary metabolites from water hyacinth, particularly terpenoids and alkaloids, have a cytotoxic effect on cancer cells by inducing apoptosis 13.

This current study utilized in silico approach; drug-likeness screening, molecular docking, proteinligand interactions profiling, and ADMET evaluation to assess the inhibitory potential of compounds present in Eichhornia crassipes for cancer treatment with the targets CDK4/6.

MATERIAL AND METHODS

Ligands selection

This study conducted a comprehensive literature review to select the bioactive compounds present in *Eichhornia crassipes*. Fifty-seven (57) bioactive compounds were selected from the plant ¹³⁻¹⁴ and palbociclib and ribociclib are used as the reference drugs. **Table 1** presents a selection of bioactive compounds from the plant alongside control drugs. Through PubChem, a web-based chemical repository (https://pubchem.ncbi.nlm.nih.gov/compound/)³⁸, we obtained key identifiers and structural information, including PIDs, SDF files, and SMILES strings.

Targets selection

CDK4/6 are the target proteins, and they were selected using literature ¹⁵⁻¹⁶. The structural data for CDK4 (PDB: 2W96) and CDK 6 (PDB: 1XO2) were retrieved from the RCSB Protein Data Bank (www.rcsb.org)¹⁷, providing 3D crystallographic information in the form of PDB. Figure 1a and b shows the structures of CDK 4 and 6 respectively.

Drug likeness screening

Utilizing the SwissADME online server

(http://swissadme.ch/) 18 and canonical SMILES, druglikeness screening was performed on 57 bioactive compounds and 2 control drugs. The analysis revealed 39 compounds adhering to Lipinski's rule 19-21, albeit

potentially violating other criteria (Veber ²², Ghose ²³, Egan 24, and Muegge 25); these were selected for molecular docking alongside control drugs.

Targets preparation

ISSN: 2357-0547 (Print)

ISSN: 2357-0539 (Online)

Using Schrodinger Suite's Protein Preparation Wizard, the 3D structure of CDK4/6 underwent cleaning and preparation (Schrodinger suite 2022, v 13.4). This process involved removing co-crystallized ligands and waters, adding hydrogen atoms, and assigning bond orders, partial charges, and atom types. The proteins were minimized and saved in PDB format for further analysis. The residues in the ATP binding site of CDK4/6 are identified from literature survey 16, 26.

Molecular docking

The docking analysis was conducted using Glide module of Schrodinger suite (Schrodinger suite 2022, v 13.4). To define the binding region, a grid enclosing the catalytic pocket of the protein targets was constructed with center dimension x: 1.39, y: 37.15, z: 139.15 for 1XO2 and x: -0.9, y: -1.24, z: 74.5 for 2W96.

(a) CDK4

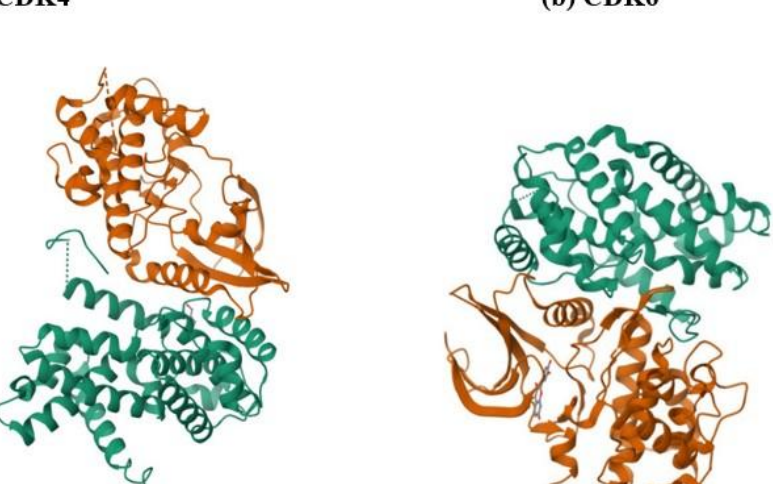


Figure 1. Structure of CDK4 and CDK6 (from PDB)

RESULTS

Drug-likeness screening

The screening results of drug-likeness bioactive compounds and reference drugs (CID 5330286 and CID 44631912) are shown in **Table 1**. Out of 57 compounds, 39 passed the Lipinski rule of five while the remaining 18 compounds violated the rule and were eliminated from the study. Compounds meeting the

The following amino acids Ile 12, Gly 13, Val 14, Gly 15, Val 20, Ala 33, Lvs 35, Val 72, Phe 93, Glu 94, His 95, Val 96, Asp 99, Arg 101, Thr 102, Glu 144, Asn 145, Leu 147, and Asp 158 for CDK4 while Lys 43, Glu 61, Asp 163, Val 101, Asp 104, Gln 149, Ile 19, Val 127, Ala 41, Phe 98, His 100, Gln 103, Leu 152, and Ala 162 for CDK6, identified through literature review 26 as residing within the binding pocket of the target proteins, were selected for molecular docking analysis. 39 compounds and 2 reference drugs were docked with standard precision and flexible docking in the catalytic site of the protein targets. The force field used was OPLS4. The compounds with lower binding energy compared with the reference drugs were subjected to further analysis.

Molecular interaction analysis

The interactions between the proteins and the hit compounds were visualized using the Ligand Interaction workflow of Schrodinger suite to decipher hydrogen bond, hydrophobic, and other interactions.

ADMET evaluation

Utilizing the ADMETLab online server (https://admetlab3.scbdd.com³⁶, we evaluated the ADMET profiles of hit compounds and control drugs to forecast their pharmacokinetic behavior.

(b) CDK6

criteria, along with control drugs, were advanced to molecular docking simulations with CDK4/6.

Molecular docking and interaction analysis of CDK4/6 and ligands

Table 2 shows the docking results of the top 8 ligands and control drugs with the amino acid residues used to interact with the target proteins. CID 5280666, CID 5280343, and CID 5280445 bind to CDK6 with

binding energies of -10.4, -10.3, and -10.2 kcal/mol respectively compared with the control drug CID 44631912 with -10.1 kcal/mol binding energy. CID 5280443, CID 3469, CID 689043, CID 5281691, and CID 10742 bind to CDK4 with binding energies of -5.8, -5.3, -5.2, -5, and -4.9 kcal/mol respectively while the control drug CID 5330286 has -4.8 kcal/mol binding energy. Figure 2 illustrates the interaction of CID 5280666, CID 5280343, CID 5280445, and CID 44631912 with CDK6. CID 5280666 interact using the amino acids Gln 149, Asp 104, Val 101 (2), Glu 61, His 100, and Lys 43 via 7 hydrogen bonds and Phe 98 through π stacking. CID 5280343 interact with the amino acids Gln 149, Asp 104, Val 101 (2), Glu 61, His 100, Asp 163, and Lys 43 through 8 hydrogen bonds. CID 5280445 interacts using the amino acids Gln 149, Asp 104, Val 101 (2), Glu 61, His 100, and Lys 43 via 7 hydrogen bonds. CID 44631912 interact using His 100, and Val 101 (2) through 3 hydrogen bonds. Figure 3 illustrates the interaction of CID 5280443, CID 3469, CID 689043 CID 5281691, CID 10742, CID 5330286 with CDK4. CID 5280443 interact with the amino acids Arg 101 (2), and Asp 158 via 3 hydrogen bonds. CID 3469 interact using Gly 15, Lys 35, and Asn 145, and Asp 158 via 4 hydrogen bonds, and Lys 35 via a salt bridge. CID 689043 interact using Val 14, and Asp 158 (2) via 3 hydrogen bonds, and Arg 101 via a salt bridge. CID 5281691 interact using Arg 101 (2), and Asp 158 (2) via 4 hydrogen bonds. CID 10742 interact using Val 14, Arg 101, and Asp 158 through 3 hydrogen bonds. CID 5330286 interact using Thr 177 via a hydrogen bond.

ADMET study

The ADMET profiles of control drugs and drug candidates are displayed in **Table 3**. For absorption and distribution, human intestinal absorption (HIA), P-

glycoprotein substrate, blood brain barrier (BBB), and plasma protein binding (PPB) are recognized as pharmacological metrics, respectively. For metabolism, CYP450 1A2, CYP450 2C19, CYP450 2C9, CYP450 2D6, and CYP450 3A4 inhibitors are considered. In addition, for excretion, T1/2 (drug half-life) was selected and ames toxicity, carcinogenicity, rat oral acute toxicity, drug-induced liver injury (DILI), human hepatotoxicity (H-HT), respiratory toxicity, human ether-a-go-go (hERG) blockers, and SR-p53 are considered for toxicity. The test compounds and control drugs exhibited a good absorption profile of HIA and P-glycoprotein substrate. All test compounds including reference drugs were suggested to be permeable to the blood-brain barrier. CID 3469, CID 10742, CID 689043, and control drugs showed PPB value below 90% as displayed in **Table 3.** For metabolism, all compounds including the control drugs are non-inhibitors of Cyp450 2C19 and 2C9 excluding CID 5281691 and CID 5280666 which are inhibitors. All compounds and the control drugs are inhibitors of Cyp450 1A2 excluding CID 3469, CID 10742, and CID 689043. CID 5280443, CID 5281691, CID 5280445, CID 5280666, and CID 5280343 are inhibitors of Cyp450 3A4. The inhibitors of Cyp450 2D6 are CID_5280443, CID 5280445, and CID 5280666. The T1/2 values range from 0.573 to 2.456. All the compounds are not hERG blockers while the control drugs are hERG blockers. All the compounds including the control drugs are carcinogenic excluding CID 3469, CID 10742, and CID_689043. The control drugs and CID 689043 are toxic to human liver. The control drugs and test compounds can cause drug-induced liver injury excluding CID 3469. All test compounds and control drugs excluding CID 689043 are toxic to the respiratory tract (as shown in Table 3).

Table 1. Screening results of drug-likeness of bioactive compounds and control drugs using the SwissADME web tool

S/ N	Molecule	Formula	MW	XLOG P	TPSA	Lipinski #Violation s	Ghose #Violation s	Veber #Violation s	Egan #Violation s	Muegge #Violation s	Bioavailabilit y Score
1	CID_14545912 5	C17H22O6	322.35	3.39	100.9	0	0	1	0	0	0.56
2	CID 785	C6H6O2	110.11	0.59	40.46	0	3	0	0	1	0.55
3	CID 2266	C9H16O4	188.22	1.57	74.6	0	0	0	0	1	0.85
4	CID_1057	C6H6O3	126.11	0.52	60.69	0	3	0	0	1	0.55
5	CID_10333	C7H8O2	124.14	1.65	40.46	0	3	0	0	1	0.55
6	CID_5054	C6H6O2	110.11	0.8	40.46	0	3	0	0	1	0.55
7	CID_11843	C7H8O2	124.14	1.58	40.46	0	3	0	0	1	0.55
8	CID_289	C6H6O2	110.11	0.88	40.46	0	3	0	0	1	0.55
9	CID_135	C7H6O3	138.12	1.58	57.53	0	3	0	0	1	0.85
10	CID_3469	C7H6O4	154.12	1.74	77.76	0	3	0	0	1	0.56
11	CID_689043	C9H8O4	180.16	1.15	77.76	0	0	0	0	1	0.56
12	CID_637542	C9H8O3	164.16	1.46	57.53	0	0	0	0	1	0.85
13	CID_445858	C10H10O4	194.18	1.51	66.76	0	0	0	0	1	0.85
14	CID_8468	C8H8O4	168.15	1.43	66.76	0	0	0	0	1	0.85
15	CID_10742	C9H10O5	198.17	1.04	75.99	0	0	0	0	1	0.56
16	CID_370	C7H6O5	170.12	0.7	97.99	0	2	0	0	1	0.56
17	CID_72	C7H6O4	154.12	1.15	77.76	0	3	0	0	1	0.56
18	CID_338	C7H6O3	138.12	2.26	57.53	0	3	0	0	1	0.85
19	CID_5281702	C17H14O7	330.29	3.07	109.36	0	0	0	0	0	0.55
20	CID 5281604	C16H12O7	316.26	1.32	120.36	0	0	0	0	0	0.55

ISSN:	2357-0547 (Print)	
ISSN:	2357-0539 (Online))

21	CID_5280445	C15H10O6	286.24	2.53	111.13	0	0	0	0	0	0.55
22	CID_5280443	C15H10O5	270.24	3.02	90.9	0	0	0	0	0	0.55
23	CID_5280666	C16H12O6	300.26	3.1	100.13	0	0	0	0	0	0.55
24	CID_5280343	C15H10O7	302.24	1.54	131.36	0	0	0	0	0	0.55
25	CID_5280863	C15H10O6	286.24	1.9	111.13	0	0	0	0	0	0.55
26	CID_439246	C15H12O5	272.25	2.52	86.99	0	0	0	0	0	0.55
27	CID_10168	C15H8O6	284.22	2.23	111.9	0	0	0	0	0	0.56
28	CID_10207	C15H10O5	270.24	1.82	94.83	0	0	0	0	0	0.55
29	CID 3034034	C20H24N2O	324.42	2.88	45.59	0	0	0	0	0	0.55
	_	2					-	-	-	-	
30	CID_5324289	C19H21NO3	311.37	2.2	30.93	0	0	0	0	0	0.55
31	CID_89594	C10H14N2	162.23	1.17	16.13	0	0	0	0	1	0.55
32	CID_5284371	C18H21NO3	299.36	1.14	41.93	0	0	0	0	0	0.55
33	CID_10235	C11H14N2O	190.24	0.18	34.03	0	0	0	0	1	0.55
34	CID_10128821	C21H26N2O	354.44	2.48	65.56	0	0	0	0	0	0.55
	8	3					Ü	O	Ü	O	
35	CID_85771	C16H35O3P	306.42	5.19	56.34	0	1	1	0	1	0.55
36	CID_570675	C14H14O	198.26	3.03	20.23	0	0	0	0	2	0.55
37	CID_5281691	C16H12O7	316.26	1.87	120.36	0	0	0	0	0	0.55
38	CID_10083	C18H21NO	267.37	3.04	32.26	0	0	0	0	0	0.55
39	CID_26905	C11H8O3	188.18	2.28	54.37	0	0	0	0	1	0.55
40	CID 5330286	C24H29N7O	447.53	1.81	105.04	0	1	0	0	0	0.55
	_	2						0		0	
41	CID_44631912	C23H30N8O	434.54	2.19	91.21	0	1	0	0	0	0.55

Table 2. Binding affinity scores, H-bond, π stacking, and π cation interaction of the hit compounds and control drugs with CDK4/6

S/N	PUBCHEM CID Binding affinity (kcal/mol)		Hydrogen bond	π stacking	Salt bridge	
	CDK4					
1	5280443	-5.8	Arg 101 (2), Asp 158	-	-	
2	3469	-5.3	Gly 15, Lys 35, Asn 145, Asp 158	-	Lys 35	
3	689043	-5.2	Val 14, Asp 158 (2)	_	Arg 101	
4	5281691	-5	Arg 101 (2), Asp 158 (2)	-	-	
5	10742	-4.9	Val 14, Arg 101, Asp 158	-	-	
6	5330286 (control)	-4.8	Thr 177	-	-	
	CDK6					
7	5280666	-10.4	Gln 149, Asp 104, Val 101 (2), Glu 61, His 100,	Phe 98	-	
			Lys 43			
8	5280343	-10.3	Gln 149, Asp 104, Val 101 (2), Glu 61, His 100,	-	-	
			Lys 43, Asp 163			
9	5280445	-10.2	Gln 149, Asp 104, Val 101 (2), Glu 61, His 100,	-	-	
			Lys 43			
10	44631912 (control)	-10.1	His 100, Val 101 (2)	-	-	

Table 3. ADMET profiling of drug candidates and control drugs

ADMET	CID_53302	CID_52804	CID_34	CID_107	CID_52816	CID_6890	CID_44631	CID_52804	CID_52806	CID_52803
models	86	43	69	42	91	43	912	45	66	43
Absorption										
&										
distribution										
P-										
glycoprotein		-		-					-	
substrate										
HIA					-	-				
BBB										
PPB	80.60%	96.50%	50.90%	76.50%	98.30%	64.70%	65.60%	97.60%	97.50%	98.70%
Metabolism										
CYP450 1A2	+++	+++			+++		+++	+++	+++	+++
inhibitor										
CYP450										
2C19									++	
inhibitor										
CYP450 2C9					++					_
inhibitor										
CYP450 2D6		+++						+	+++	
inhibitor										
CYP450 3A4		+++			+++			+++	+++	+++
inhibitor										
Excretion	0.604	1 202	1.500	2.456	1.46	2.05	0.550	1 272	1.262	1.506
T1/2	0.694	1.203	1.729	2.456	1.46	2.07	0.573	1.373	1.362	1.586
Toxicity										
Ames toxicity	+	+	-	-	+		-	+	+	+

Carcinogenic ity	++	++		-	+		+	+	++	+
Rat oral acute toxicity	+	+	-	-	-		++	+	-	-
H-HT	+++	-	-	-	-	+	+++	-	-	-
DILI	+++	++	-	+	++	+	+++	++	++	++
hERG blockers	+++						+++			
Respiratory toxicity	+++	++	++	+	+	-	+++	++	++	+
SR-p53	-	+++			++			++	+++	++

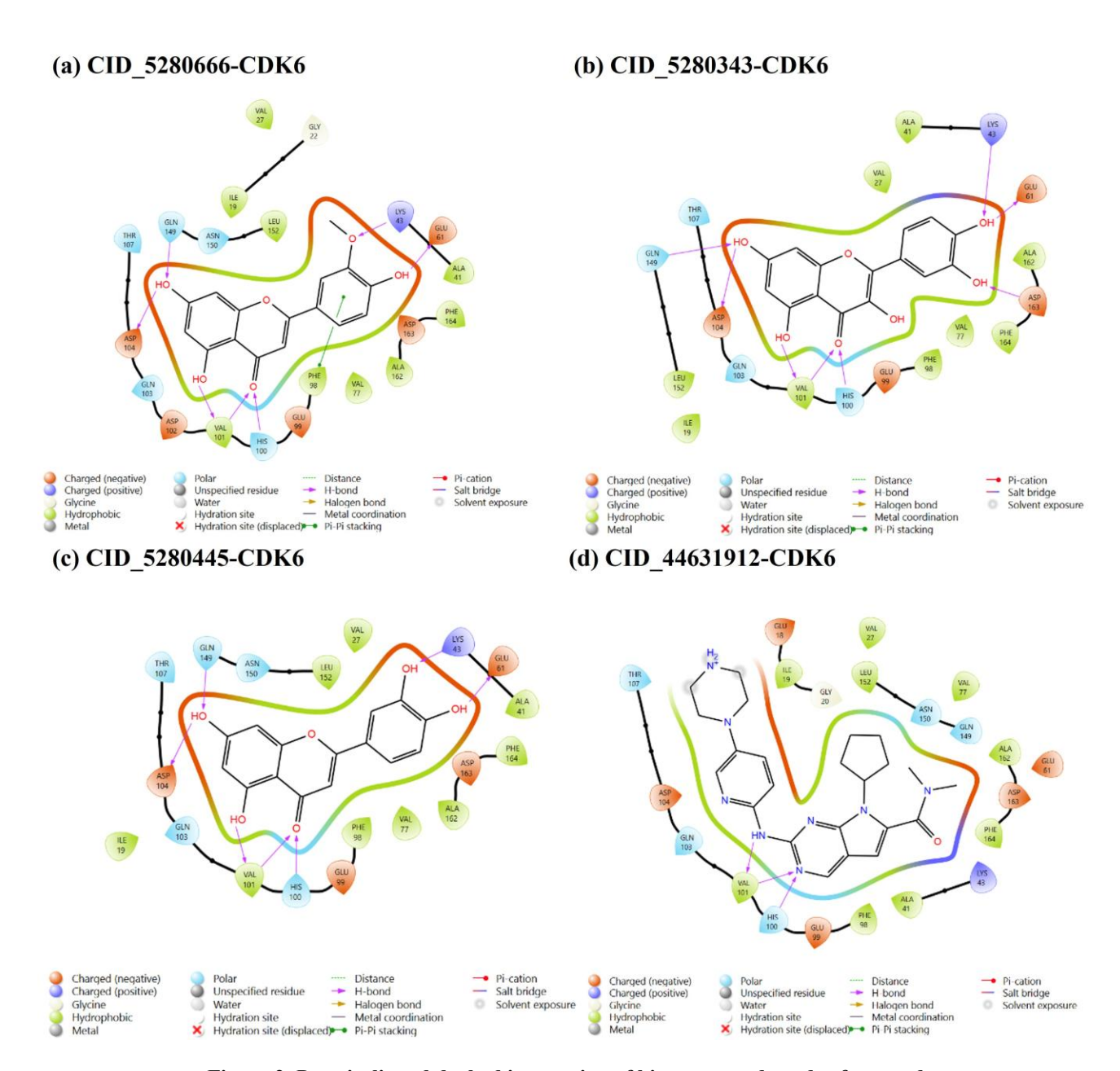


Figure 2. Protein-ligand docked interaction of hit compounds and reference drug

DISCUSSION

Due to the intricate, resource-intensive, and prolonged nature of drug discovery and development. there is a pressing need for efficient and cost-effective strategies to accelerate the identification of promising therapeutic candidates²⁷. Molecular modeling has emerged as a transformative approach in overcoming drug discovery research hurdles. Specifically, molecular docking, MD simulation, and ADMET modeling have become essential tools, streamlining lead identification for experimental testing ²⁷. Molecular modeling offers a promising approach to accelerate drug discovery, allowing researchers to identify potential small molecule therapeutics that can effectively inhibit target receptors and manage or treat diseases ²⁸. Molecular docking is an in-silico technique that aims to accurately predict protein-ligand interactions, identifying binding sites and estimating affinity, with reliable methods distinguishing between binding and non-binding regions²⁹. The success of a drug depends on both its biological potency and favorable ADMET profile. Following silico molecular docking predictions, potential drug candidates must demonstrate optimal pharmacokinetic properties, including absorption, distribution, metabolism, elimination, and non-toxicity 30.

The drug-likeness properties of bioactive compounds and control drugs were assessed with the parameters: Molecular weight, Topological Polar Surface Area (TPSA), XLogP, Lipinski, Veber, Ghose, Egan, and Muegge rules, and Bioavailability score (Table 1). By analyzing a drug's pharmacological or biological properties, Lipinski's rule of five determines if it may be administered orally. According to Lipinski's rule of five, a drug molecule has good draggability and is suitable for use as a drug if its molecular weight is less than 500 Daltons ²⁰. All the 39 bioactive compounds have molecular weight within the Lipinski's range as shown in Table 1 including reference drugs and can be taken orally. The drug's molecular weight also affects its capacity to heal. When a compound's molecular weight rises above a certain threshold, its surface area increases, and its penetrability decreases ¹⁹. The permeability of drugs is further influenced by TPSA and Molecular Lipophilicity Potential (XlogP value), which together define oral bioavailability. XLogP, the logarithm of the n-octanol/water partition coefficient, is a key indicator of molecular lipophilicity, affecting permeability across biological membranes and hydrophobic interactions with receptors, transporters, plasma proteins, and enzymes ³⁷. According to Lipinski's rule of five, a drug compound prefers hydrophilic (polar) media if LogP is less than 5, and hydrophobic (non-polar) medium if LogP is greater than 5 20. In this study, 38 compounds and reference drugs have LogP value that is less than 5 and this indicates that the compounds interact well in hydrophilic (polar) media. CID 85771 interact well in hydrophobic media with 5.19 LogP value.

Molecular docking serves as a computational tool to predict the optimal binding conformations and inhibitory effects of protein-ligand complexes, driven by intermolecular interactions 31. Interactions between ligands and proteins are essential for biological processes, and binding and dissociation are two important mechanisms. Longer time spans between these occurrences are linked to stronger binding affinities. A better understanding of atomistic interactions, such as ligand binding and dissociation from catalytic sites, can be obtained by studying protein-ligand interactions³. This study utilizes molecular docking to evaluate the binding affinity of compounds to the target proteins' catalytic pocket, with ligands ranked according to descending order of affinity. The analysis identified optimal docking orientations and critical interacting residues crucial for ligand binding. The docking result revealed that CID 5280666, CID 5280343, and CID 5280445 had better binding affinity compared to CID 44631912 against CDK6. It also showed that CID 5280443, CID 3469, CID 689043, CID 5281691, and CID 10742 had superior binding affinity compared to CID 5330286 against CDK4. Molecular docking simulations predict the binding conformation of a ligand to a protein based on geometric and electrostatic complementarity 32. The docking score, measured in kcal/mol, estimates the strength of ligand-protein interactions, with lower negative energies (E) indicating stronger binding. Therefore, the compounds with superior binding affinity may possess some anticancer properties by inhibiting the targets. The ligands interact with the amino acid residues Ile 12, Gly 13, Val 14, Gly 15, Val 20, Ala 33, Lys 35, Val 72, Phe 93, Glu 94, His 95, Val 96, Asp 99, Arg 101, Thr 102, Glu 144, Asn 145, Leu 147, and Asp 158 at the active pocket of CDK4 and Lys 43, Glu 61, Asp 163, Val 101, Asp 104, Gln 149, Ile 19, Val 127, Ala 41, Phe 98, His 100, Gln 103, Leu 152, and Ala 162 at the catalytic region of CDK6. The compounds' interactions with targets indicate potential inhibitory activity, with hydrogen bonding, pi stacking, and salt bridge interactions emerging as key factors in protein-ligand binding.

Identifying potent drug candidates with tolerable ADMET profiles is one of the most crucial objectives of an effective drug development procedure. Recently, computational approaches have emerged to predict the pharmacokinetic profile, bioavailability, toxicity, and safety of novel compounds in humans, reducing reliance on resource-intensive experiments³³. To accomplish this, Palbociclib and Ribociclib (as shown in **Table 3**) were used to compare the ADMET profiles of the eight promising inhibitors found through our investigation. Our goal is to exclude drugs that, when compared to the reference inhibitors, have higher or undesirable ADMET profiles. A potent small ligand must achieve high concentrations at its target site in the body to exhibit efficacy and maintain its bioactive form

for a sufficient duration to exert its therapeutic effects 34 . For categorization model predictions, a six-tiered symbol system is employed, where probability ranges are represented as follows: --- (0-0.1), -- (0.1-0.3), - (0.3-0.5), + (0.5-0.7), +++ (0.7-0.9), +++ (0.9-1.0), encompassing endpoints such as PPB and HIA. The symbols "---" or "--" indicate a molecule that is appropriate or harmless, while "+ + + "or "+ + " often indicates a molecule posing increased safety concerns or liability for adverse outcomes 33 .

The data presented in Table 3 show that both the test compounds and control drugs exhibited exceptional absorption characteristics with "---" or "--" value of HIA excluding CID 5281691 and CID 689043 with moderate profiles of "-" and P-glycoprotein substrate with "---" or "--" excluding CID 5280443, CID 10742, and CID 5280666 with moderate profiles of "-". A study by Lin and Yamazaki (2003) 35 revealed that a member of the ABC (ATP-binding cassette) protein family, P-glycoprotein, plays a crucial role in efflux, preventing bioaccumulation cellular compounds and modulating their biological effects. This indicates that the drug candidates exhibit favorable properties for therapeutic application. All test compounds including reference drugs showed profiles with "---" or "--" values of BBB suggesting improved delivery and efficacy in the central nervous system due to enhanced blood-brain barrier penetration. PPB is crucial for determining drug pharmacokinetics and pharmacodynamics. PPB influences oral bioavailability and affects the free concentration of a drug when bound to serum proteins. For effective therapy, a drug should exhibit plasma protein binding below 90%. High protein binding can limit therapeutic efficacy ³². With a PPB value below 90%, CID 3469, CID 10742, CID 689043, and control drugs demonstrate promising therapeutic potential.

In terms of metabolism, the Cyt p450 families are identified as essential parameters. The observed inhibition of these enzyme families (denoted by +++/++) may imply that the hit compounds could interact with other medications, leading to accumulation in the body³³. All compounds including the control drugs excelled in Cyt p450 2C19 and Cyt p450 2C9 (excluding CID 5281691 and CID 5280666). As shown in table 3, CID 3469, CID 10742, and CID 689043 are the drug candidates with the best metabolic profiles of "---" or "--" values. In contrast, the worst Cyt p450 profile CID 5280666. compound is An essential pharmacokinetic parameter in the excretion section is T1/2, or clearance. This parameter, coupled with the volume of distribution, consequently, establishes the frequency of dosing and a drug's half-life. Levels in the range of 0 to 0.3 exhibit outstanding empirical decision, output levels between 0.3 and 0.7 are considered average, and values over 0.7 suggest a suboptimal excretion pattern ³³. Disappointingly, none of the hit compounds demonstrated satisfactory disposition profiles, characterized by scores of 1.203 to 2.456.

Lastly, a critical pharmacological factor that may influence a drug's approval following clinical trials is its pharmacodynamics. In order to achieve this, we determined eight ADMET endpoints (respiratory toxicity, rat oral acute toxicity, hERG blockers, DILI, carcinogenicity, ames toxicity, H-HT and SR-p53) that may be used to gauge how well the promising inhibitors perform in clinical trials. The results showed that hERG is the only parameter in which the hit compounds displayed significant and consistent score excluding control drugs with poor output. In the parameters H-HT, rat oral acute, and ames toxicity, all compounds showed moderate toxicity excluding CID 689043 which showed excellent in rat oral acute toxicity, CID 5281691 and CID 5280343 showed poor ames toxicity, and CID 689043 with excellent ames toxicity profile. All hit compounds including the control drugs showed poor respiratory toxicity except CID 689043 with moderate output. Across other pharmacodynamics models, the drug candidates exhibited diverse response profiles.

In conclusion, key findings from this ADMET study (**Table 3**) are that CID_3469, CID_10742, and CID_689043 emerged with favorable pharmacokinetic/pharmacodynamics properties, indicating potential therapeutic advantages over existing control drugs. However, other drug candidate's ADMET profiles can be modified for suitable efficacy.

CONCLUSION

This study investigated the therapeutic potential of some bioactive compounds present in water hyacinth against CDK4/6 for cancer treatment. Out of 57 selected compounds, 39 compounds passed the drug-likeness screening and were subjected to docking analysis. Eight hit compounds were found to have superior binding affinity in comparison with reference drugs and ADMET study was conducted on the drug candidates and reference drugs. Three drug candidates CID_3469, CID_10742, and CID_689043 showed better ADMET profiles than the control drugs while the remaining five may show equal output. This study requires further optimization and experimental evaluation of the hit compounds for validation before subjecting to clinical trials.

Funding Acknowledgement

No external funding was received.

Conflict of interest

The authors declare no conflict of interest regarding this publication.

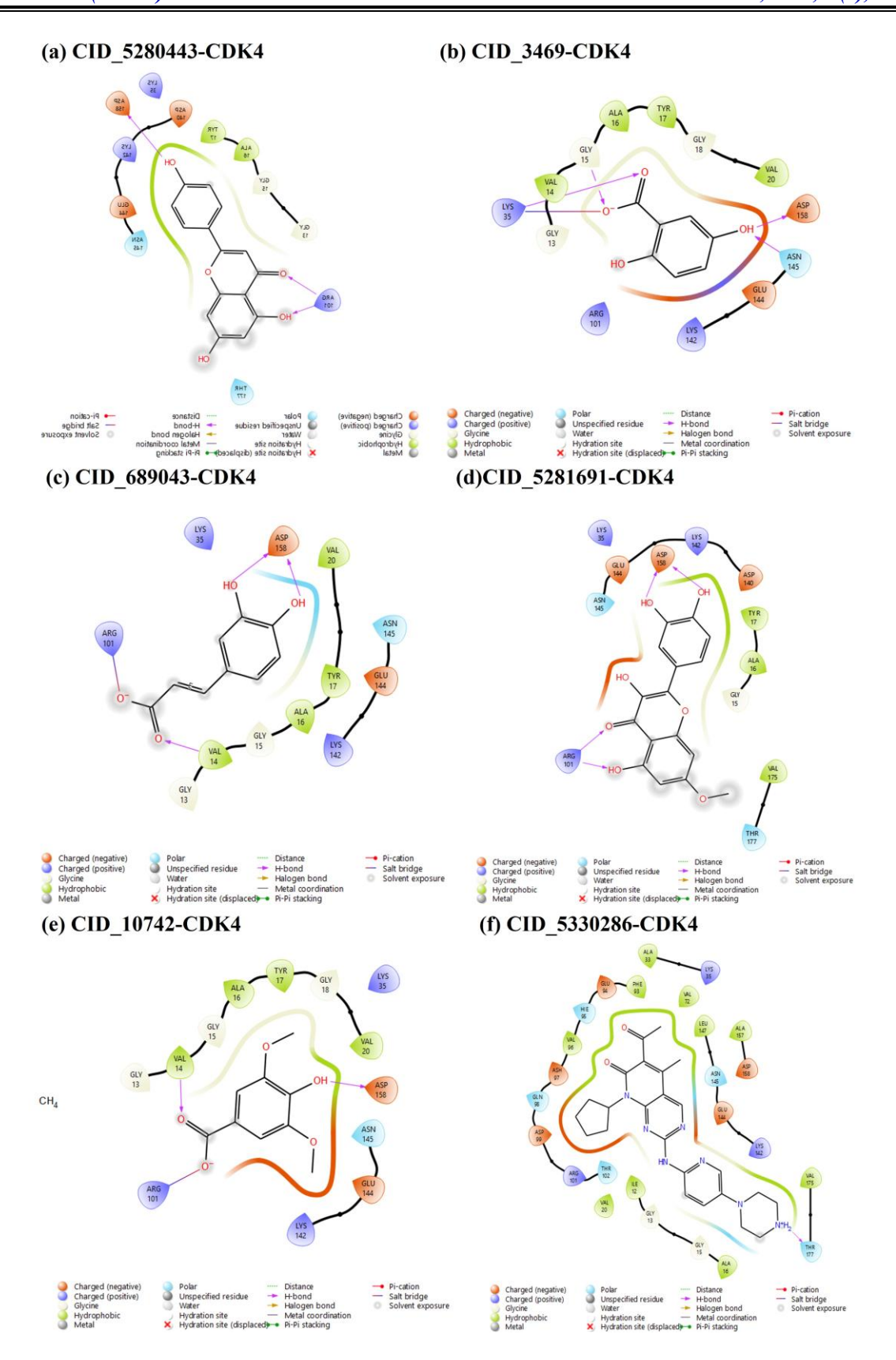


Figure 3. Protein-ligand docked interaction of hit compounds and reference drug

REFERENCES

ISSN: 2357-0547 (Print)

ISSN: 2357-0539 (Online)

- 1. Ashiru, M.A.; Ogunyemi, S.O.; Temionu, O.R.; Ajibare, A.C.; Cicero-Mfon, N.C.; Ihekuna, O.A; Jagun, M.O.; Abdulmumin, L.; Adisa, Q.K.; Asibor, Y.E.; Okorie, C.J.; Lawal, M.O.; Babalola, M.O.; Abdulrasaq, I.T.; Salau, L.B.; Olatunji, I.O.; Bankole, M.A.; Daud, A.B.; Adeyemi. A.O. Identification of EGFR inhibitors as potential agents for cancer therapy: pharmacophore-based modeling, molecular docking, and molecular dynamics investigations. *J of Mole Mod.* **2023**, *29*, 128 https://doi.org/10.1007/s00894-023-05531-6
- Bray, F.; Laversanne, M.; Sung, H.; Ferlay, J.; Soerjomataram, I.; Siegel, R.L.; Torre, L.A.; Jemal, A. Global cancer statistics 2022: GLOBOCAN estimates of incidence and mortality worldwide for 36 cancers in 185 countries. *CA Can J Clin.* 2024, 74 (3), 229-263. https://doi.org/10.3322/caac.21834
- 3. Mahmood, K.; Kamaljot, S.; Sara, K.; Basharat, A.; Aneela, K.; Sun, Y. Computational exploration of allosteric inhibitors targeting CDK4/CDK6 proteins: a promising approach for multi-target drug development. *J of Bio Struct and Dyn.* **2024**, https://doi.org/10.1080/07391102.2023.2300121
- 4. Rakhi, S. A.; Asaduzzaman, M.; Nasin, N; Md Khademul Islam, A. B. M. An in silico evaluation of CDK Inhibitors targeting BCL2, TS and mTOR. *Asian J of Med and Bio Res.* **2021**, *7* (2), 126-131. https://doi.org/10.3329/ajmbr.v7i2.54991
- 5. Łukasik, P.; Załuski, M.; Gutowska, I. Cyclin-Dependent Kinases (CDK) and their role in diseases development–review. *Int J of Mole Sci.* **2021**, *22* (6), 2935. https://doi.org/10.3390/ijms22062935
- Baker, S.J.; Poulikakos, P.I.; Irie, H.Y.; Parekh, S.; Reddy, E.P. CDK4: a master regulator of the cell cycle and its role in cancer. *Gene Cancer* 2022, 25 (13), 21-45. doi: 10.18632/genesandcancer.221. PMID: 36051751; PMCID: PMC9426627.
- Ding, L.; Cao, J.; Lin, W.; Chen, H.; Xiong, X.; Ao, H.; Yu, M.; Lin, J.; Cui, Q. The roles of cyclin-dependent kinases in cell-cycle progression and therapeutic strategies in human breast cancer. *Int J of Mole Sci*, 2020, 21 (6), 1960.
- Wang, X.; Zhao, S.; Xin, Q.; Zhang, Y.; Wang, K.; Li, M. Recent progress of CDK4/6 inhibitors' current practice in breast cancer. *J Cancer Gene Therapy*. 2024, 31, 1283-1291 https://doi.org/10.1038/s41417-024-00747-x
- Jin, H.; Wang, L.; Bernards, R. Rational combinations of targeted cancer therapies: background, advances and challenges. *Nat Rev Drug Discov.* 2023, 22, 213-234. https://doi.org/10.1038/s41573-022-00615-z
- 10. Abba, A.; Sankarannair, S. Global impact of water hyacinth (*Eichhornia Crassipes*) on rural

- communities and mitigation strategies: a systematic review. *Envir Sci Pollut Res.* **2024**, *31*, 43616–43632. https://doi.org/10.1007/s11356-024-33905-7
- 11. Koley, A.; Bray, D.; Banerjee, S.; Sarhar, S.; Thahur, R.G.; Hazra, A.K.; Balachandran, S. Water hyacinth (*Eichhornia crassipes*) a sustainable strategy for heavy metals removal from contaminated waterbodies. *Int Bio of Tox Metal (loid) s.* **2022**, 95-114. CRC Press.
- 12. Rabiepour, A.; Babakhani, A.; Zakipour R.E. Effect of extraction methods on the antioxidant properties of water hyacinth, *Eichhornia crassipes*. *Cas J of Environ Sci.* **2024**, 1-19. https://doi.org/10.22124/CJES.2024.8015
- Ben-Bakrim, W.; Ezzariai, A.; Karouach, F.; Sobeh, M.; Kibret, M.; Hafidi, M.; Yasri, A. Eichhornia crassipes (Mart.) Solms: A comprehensive review of its chemical composition, traditional use, and value-added products. Front in Pharm. 2022, 13, 842511.
- 14. Pottail, L.; Shubashini, K.S.; Ponnusamy, J. Secondary metabolites of *Eichhornia crassipes* (water hyacinth): A review (1949 to 2011). *Nat Prod Comm.* **2012**. *7* (9).
- 15. Philip, J.; Day, A.C.; Ian, J.; Tickle, M.O.; Joe, E.C.; Finn, P.H.; Rachel, L.M.; Jeff, Y.; Rajiv, C.; Christoph, L.; Harren. *J Cry struct of hum CDK4 in complex with a D-type cyclin.* **2009**, *17* (106), 4166–4170.
- www.pnas.org_cgi_doi_10.1073_pnas.0809645106
 16. Heshu, L.U.; Debbie, J.; Chang, B.B.; Laurent, M.; Ursula, S. Crystal structure of a human cyclin-dependent kinase 6 complex with a flavonol inhibitor, fisetin. *J Med Chem.* **2005**, *48*, 737-743. https://doi.org/10.1021/im049353p
- 17. Berman, H.M.; Westbrook, J.; Feng, Z.; Gilliland, G.; Bhat, T.N.; Weissig, H.; Shindyalov, I.N.; Bourne, P.E. The Protein Data Bank Nucleic Acids. *J Res.* **2000**, *28*, 235-242.
- 18. Daina, A.; Michielin, O.; Zoete, V. SwissADME: a free web tool to evaluate pharmacokinetics, druglikeness and medicinal chemistry friendliness of small molecules. *Sci Rep.* **2017**. *7*, 42717. https://doi.org/10.1038/srep42717
- 19. Lipinski, C.A. Drug-like properties and the causes of poor solubility and poor permeability. *J Pharmacol Toxicol Meth.* **2008**, *44*, 235–249.
- Lipinski, C.A.; Lombardo, F.; Dominy, B.W.; Feeney, P.J. Experimental and computational approaches to estimate solubility and permeability in drug discovery and development settings. *Adv Drug Delivery Rev.* 2001, 46 (1-3), 3–26. https://doi.org/10.1016/S0169-409X(00)00129-0.
- 21. Lipinski, C. Rule of five in 2015 and beyond: Target and ligand structural limitations, ligand chemistry structure and drug discovery project decisions. *Adv*

- Drug Deliv Rev. **2016**, 101, 34–41. Veber, D.F.; Johnson, S.R.; Cheng, H.Y.; Smith, B.R.; Ward, K.W.; Kopple, K.D. Molecular properties that influence the oral bioavailability of drug candidates. *J Med Chem.* **2002**, 45, 2615–2623.
- 22. Bickerton, G.R.; Paolini, G.V.; Besnard, J.; Muresan, S.; Hopkins, A.L.; Quantifying the chemical beauty of drugs. *Nat chem*. **2012**, *4* (2), 90–98.https://doi.org/10.1038/nchem.1243.
- 23. Egan, W. J.; Merz, K. M.; Baldwin, J. J.; Prediction of drug absorption using multivariate statistics. *J Med Chem.* **2000**, *43*, 3867–3877.
- Muegge, I.; Heald, S.L.; Brittelli, D. Simple Selection Criteria for Drug-like Chemical Matter. J Med Chem. 2001, 44, 1841–1846.
- Rondla, R.; PadmaRao, L.S.; Ramatenki, V.; Haredi-Abdel-Monsef, A.; Potlapally, S.R.; Vuruputuri, U. Selective ATP competitive leads of CDK4: Discovery by 3D-QSAR pharmacophore mapping and molecular docking approach. *J Com Bio Chem.* 2007, 71, 224-229. https://doi.org/10.1016/j.compbiolchem.2017.11.00
- Chunarkar-Patil, P.; Kaleem, M.; Mishra, R.; Ray, S.; Ahmad, A.; Verma, D.; Bhayye, S.; Dubey, R.; Singh, H.N.; Kumar, S. Anticancer drug discovery based on natural products: From computational approaches to clinical studies. *Biomed.* 2024, 12, 201. https://doi.org/10.3390/biomedicines12010201
- Sadybekov, A.V.; Katritch, V. Computational approaches streamlining drug discovery. *Nat J.* 2023, 673–685 https://doi.org/10.1038/s41586-023-05905-z
- 28. Mursal, M.; Ahmad, M.; Hussain, S.; Faraz Khan, M. Navigating the computational seas: A comprehensive overview of molecular docking software in drug discovery. *Intech Open.* **2024**, doi: 10.5772/intechopen.1004802
- Adelusi, T.I.; Oyedele, A.K.; Boyenle, I.D.; Ogunlana, A.T.; Adeyemi, R.O.; Ukachi, C.D.; Idris, M.O.; Olaoba, O.T.; Adedotun, I.O.; Kolawole, O.E.; Xiaoxing, Y.; Abdul-Hammed, M. Molecular modeling in drug discovery, *Inform in Med Unlock*. 2022, 29, 2352-9148, https://doi.org/10.1016/j.imu.2022.100880.
- 30. Sahu, M.K.; Nayak, A.K.; Hailemeskel, B.; Eyupoglu, O.E. Exploring recent updates on

- molecular docking: Types, method, application, limitation & future prospects. *Int J Pharm Res Allied Sci.* **2024**, *13* (2), 24-40. https://doi.org/10.51847/Une9jqjUCl.
- Akinwumi, I A.; Faleti, A. I.; Owojuyigbe, A. P.; Raji, F. M.; Alaka, O. M. In silico studies of bioactive compounds selected from four African plants with inhibitory activity against *Plasmodium falciparum* dihydrofolate teductase-Thymidylate synthase (pf DHFR-TS). J Adv Pharm Res. 2022, 6 (3), 107-122. DOI: 10.21608/aprh.2022.139794.1175.
- 32. Oyedele, A.K.; Adelusi, T.I.; Ogunlana, A.T.; Adeyemi, R.O.; Atanda, O.E.; Babalola, M.O.; Ashiru, M.A.; Ayoola, I.J.; Boyenle, I.D. Integrated virtual screening and molecular dynamics simulation revealed promising drug candidates of p53-MDM2 interaction. *J of Mole Mod.* 2022, 28, 142. https://doi.org/10.1007/s00894-022-05131-w.
- Shahbaz, M.; Imran, M.; Hussain, M.; Alsagaby, S. A.; Momal, U.; Naeem, H.; Al Jbawi, E. Curcumin: a bioactive compound with molecular targets for human malignancies. J Food Agri Imm. 2023, 34 (1). https://doi.org/10.1080/09540105.2023.2280524.
- 34. Lin, J.; Yamazaki, M. Role of P-glycoprotein in pharmacokinetics. *Clin Pharmacokinet*. **2003**, *42* (1), 59–98.
- 35. Xiang, Z.; Cheng-Kun, W.; Ai-Ping, L.; Xiang, C.; Ting-Jun, H.; Dong-Sheng, C.; ADMETlab 2.0: an integrated online platform for accurate and comprehensive predictions of ADMET properties. *Nuc Acids Res.* **2021**, *49*, 5-14.
- 36. Daria, K.; Małgorzata, J.; Małgorzata, D.; Beata, M. Study of the lipophilicity and ADMET Parameters of new anticancer diquinothiazines with pharmacophore substituents. *J Pharma.* **2024**, *17* (6), 725. https://doi.org/10.3390/ph17060725.
- 37. Kim, S.; Chen, J.; Cheng, T.; Gindulyte, A.; He, J.; He, S.; Li, Q.; Shoemaker, B. A.; Thiessen, P. A.; Yu, B.; Zaslavsky, L.; Zhang, J.; Bolton, E. E. PubChem in 2021: new data content and improved web interfaces. *Nuc Acids Res.* **2019**, *49* (D1), D1388–D1395. https://doi.org/10.1093/nar/gkaa 971.